

# GLOBAL AND LOCAL GEOSPACE MODELING IN ISTP

K. PAPADOPOULOS

*Department of Physics, University of Maryland, College Park, MD 20742, U.S.A.*

J. G. LYON

*Department of Astronomy, University of Maryland, College Park, MD 20742, U.S.A.; and  
Department of Physics and Astronomy, Dartmouth College, Hanover, NH 03755, U.S.A.*

C. C. GOODRICH, P. J. CARGILL, A. S. SHARMA and R. KULKARNI

*Department of Astronomy, University of Maryland, College Park, MD 20742, U.S.A.*

and

CL. L. CHANG and A. MANKOFSKY

*science Applications International Corporation, McLean, VA 22102, U.S.A.*

(Received 15 March, 1993)

**Abstract.** The objective of the University of Maryland ISTP theory project is the development of the analytical and computational tools, which, combined with the data collected by the space and ground-based ISTP sensors, will lead to the construction of the first causal and predictive global geospace model. To attain this objective a research project composed of four complementary parts is conducted. First the global interaction of the solar wind-magnetosphere system is studied using three-dimensional MHD simulations. Appropriate results of these simulations are made available to other ISTP investigators through the Central Data Handling Facility (CDHF) in a format suitable for comparison with the observations from the ISTP spacecrafts and ground instruments. Second, simulations of local processes are performed using a variety of non-MHD codes (hybrid, particle and multifluid) to study critical magnetospheric boundary layers, such as the magnetopause and the magnetotail. Third, a strong analytic effort using recently developed methods of nonlinear dynamics is conducted, to provide a complementary semi-empirical understanding of the nonlinear response of the magnetosphere and its parts to the solar wind input. The fourth part will be conducted during and following the data retrieval and its objective is to utilize the data base in conjunction with the above models to produce the next generation of global and local magnetospheric models. Special emphasis is paid to the development of advanced visualization packages that allow for interactive real time comparison of the experimental and computational data. Examples of the computational tools and of the ongoing investigations are presented.

## 1. Introduction

The International Solar-Terrestrial Physics (ISTP) program is the centerpiece of the current magnetospheric physics research effort. It marks the transition from scientific exploration to scientific maturity in experimental and theoretical space plasma physics. The primary objective of the program is the construction of reliable, self-consistent, quantitative, magnetospheric models, capable of cause and effect prediction. The success of the program rests on two complementary efforts: an observational effort that provides the data base on the overall flow of energy, mass, and momentum throughout geospace and an associated theoretical effort that develops the analytic and computational models on which the next generation

global magnetospheric models will be based. The elements that make feasible the goals of ISTP at the present time are the development of new, high resolution instrumentation, advances in computer hardware for data storage, dissemination, and analysis, and progress in theoretical and computational plasma physics.

The objective of the ISTP theory project in the Departments of Physics and Astronomy at the University of Maryland, College Park, is the development of the theoretical and computational foundations, which, combined with the data collected by the space and ground based ISTP sensors, will permit the construction of the first causal, predictive, global geospace models. The success of the ISTP program depends critically on the availability of dynamic computational models, that can provide a global framework for interpreting the observational data. The University of Maryland theory project emphasizes the modeling of the global magnetosphere, its local components, and the expected ionospheric response. To facilitate the comparisons with the data easy access of the simulation results to the experimental teams will be provided.

An overall picture of our project can be obtained by dividing it into two major generic areas: 'global' and 'local' studies. The global studies involve the coupling of many different regions of geospace, and describe in a zeroth order sense, the flow and dissipation of energy and overall structure of the magnetic field and plasma in a system that extends for many tens of  $R_E$ . An example of such global modeling is provided by three dimensional MHD simulations of the magnetosphere. Benchmarking and improving the global models requires simultaneous data from many spacecraft located in different regions of the magnetosphere, as well as ground based observations. Global modeling is discussed in Sections 2 and 4.

Local studies concentrate on smaller regions of geospace such as the magnetopause, the magnetotail and the bow shock, whose extent is often much smaller than 1  $R_E$ . Important issues in local studies are the determination of the local plasma transport (both along and across the magnetic field) and the stability and dissipation of currents and beams of energetic particles. The local modeling relies, predominantly, on single satellite, multi-instrument data sets, and mesoscale data from the CLUSTER array. It is most important to recognize that local processes can control the global structure by providing the anomalous transport coefficients (e.g., anomalous resistivity, viscosity, etc.) necessary for the correct global description. It is one of our goals to provide the methodology needed to merge the global and local descriptions. Section 3 addresses issues related to local modeling.

Two other important ingredients of the project are dictated by the need of the experimental groups to readily access theoretical models and predictions. To facilitate this task a data base of 3-D MHD simulation runs for relevant solar wind parameters has been developed. This data base is located at the Central Data Handling Facility (CDHF) and is readily accessible to all experimental teams. A critical ingredient of the data base is efficient visualization of the simulation results. The advances in high power workstations enabled us to develop new, multi-dimensional, advanced visualization methods that facilitate the interpretation and

data comparison of both global and local simulation results. The ultimate goal is to develop simple, ready to use packages that allow experimentalists and theorists to perform rapidly comparisons of theory with spacecraft data. These advanced visualization techniques go well beyond the traditional line plots, to fully three dimensional, interactive methods for examining the numerical simulation output along with the data. These aspects of the project are discussed in Section 5.

## 2. Global Modeling

Global MHD simulations of the Earth's magnetosphere are an important part of the ISTP theory program. Such simulations are currently the only way to obtain an overall description of the solar wind-magnetosphere-ionosphere system. There are clear limits to the applicability of MHD theory to the magnetosphere, particularly to the important boundary layers. However, MHD describes with relative accuracy, the bulk flows of energy and momentum in large areas of the system. When global MHD simulations are carried out, it is assumed that the details of the transport in boundary layers do not greatly influence the overall interaction of the different magnetospheric regions and the transport of mass, momentum, and energy among them.

The simulation of a system like the magnetosphere, with length scales ranging from hundreds of  $R_E$  to hundreds of kilometers or less, presents extreme technical challenges. Brute force resolution of the various structures is beyond current computer capabilities. An hour of simulated real time requires many hours of machine time on a  $100 \times 100 \times 100$  grid. Increasing the resolution by a factor  $f$ , increases the computer time by a factor of  $f^4$  for the best case, and for many of the commonly used algorithms by a factor of  $f^8$ . It is thus imperative to utilize, to the maximum extent possible, physical insights in performing the calculations. We have followed this idea in the design and construction of our simulation code which is pacing the current state of the art.

The simulation code has several distinctive features. The grid is computationally rectangular, but non-orthogonal and is adapted to the specific problem. Computational cells are much smaller in the near-earth region than in the far magnetosheath or the deep tail. For improved phase accuracy, high-order (8th) spatial differencing is used. To suppress the oscillations associated with high-order schemes, a nonlinear switch, based on the Partial Donor Method (PDM) of Hain (1987), is used, to change, selectively, from the basic high-order algorithm to one that does not create new extrema in the neighborhood of discontinuities. While it is difficult to quantify the gain in resolution of this numerical scheme, we note as a benchmark that the code is capable of advecting a Gaussian with 2 cell width (FWHM), essentially, without error and can resolve a shock cleanly in 1–2 cells. This and other considerations lead to an estimate of a gain factor of 3–4 in linear resolution over a simple second-order algorithm such as Lax–Wendroff.

A unique feature of this code is the ionospheric boundary condition. It is the only global MHD code which self-consistently couples the ionosphere to the magnetosphere. This is done by defining an inner boundary to the MHD simulations (usually about  $3 R_E$ ). At this inner boundary the field-aligned current is calculated from the curl of the B field given by the MHD calculation. The current is then mapped to the ionosphere, where it provides the source term for a standard height integrated, electrostatic equation for the ionospheric electric potential,  $\nabla \cdot (\Sigma \nabla \psi) = J_{\parallel}$  where  $\Sigma$  is the ionospheric conductivity tensor and  $\psi$  is the potential.  $\Sigma$  may contain both Pedersen and Hall conductivities and may also vary spatially.

Much of the exploratory work has been done on a low-resolution mesh ( $14 \times 16 \times 32$ ) which spans the region  $-100 R_E < x < 20 R_E$ ,  $\sqrt{y^2 + z^2} < 60 R_E$ . This coarse grid still provides approximately  $1 R_E$  cell size in the region of the magnetopause and produces an hour's worth of simulated magnetospheric time in somewhat less than an hour of Cray time. Results from a simulation with a westward interplanetary magnetic field are shown in Figure 1. The plasma density is shown, color coded, on north-south and east-west planes, together with the magnetic field lines traced from the dayside portion of Earth's ionosphere; the planes have been rendered semitransparent to show better the trajectories of the field lines. The density display shows the basic features of the geospace system – the bow shock, the magnetosheath, the magnetopause and the extended geomagnetic tail – and provides a spatial reference for examining the structure of the magnetic field. The field line traces show the compression and tailward sweep of the closed field lines as well as the open (reconnected) field lines originating in the north and south polar regions.

Even at this low resolution, the simulations show a number of features of the real magnetosphere (Fedder and Lyon, 1987; Fedder *et al.*, 1991, 1992). Principal among these features are the existence of Region 1 currents on closed field lines, the extension of those currents across noon for IMF with  $B_y \neq 0$ , the location of the constriction in the ionospheric plasma flow (known as the 'convective throat') with respect to noon, the generation of the cusp/mantle currents, and the generation of NBZ (northern  $B_z$ ) currents for northward IMF. Associated with NBZ currents is a decay of anti-sunward flow through the polar cap. These simulations have convincingly demonstrated the ionospheric control of the dayside reconnection rate (Fedder and Lyon, 1987).

A major advance in magnetospheric modeling has been recently achieved by greatly extending the spatial scale of the MHD simulation code. The newly achieved  $25 R_E$  to  $-300 R_E$  extent of the code allows the inclusion in the simulations of the far magnetotail region, necessary for proper representation of the global physics and for the prediction and interpretation of the GEOTAIL observations. Equally important, at the downstream boundary of the code at  $-300 R_E$ , the plasma flow is consistently supersonic and super-Alfvénic, thus eliminating the influence of the artificial downstream boundary conditions on the physics. This was a major drawback in simulations extending less than  $100 R_E$  downstream. The qualitative

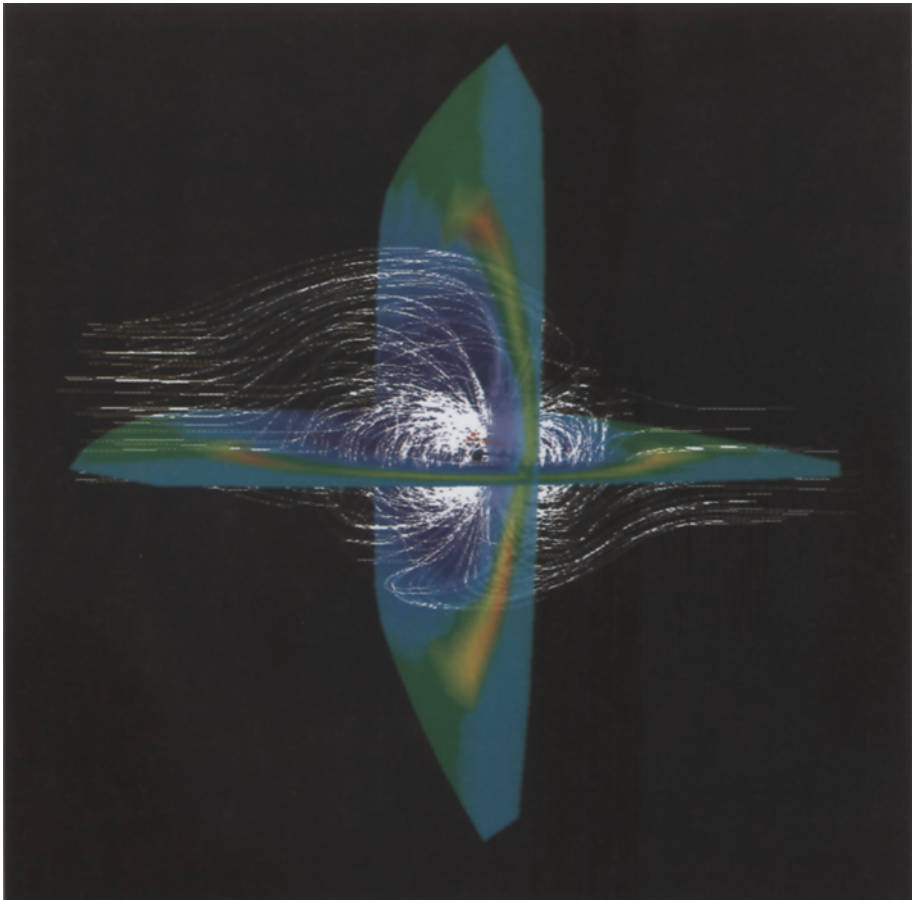


Fig. 1. Density and magnetic field lines originating from the Earth's dayside hemisphere from an MHD simulation with a westward IMF; the Sun is to the right and north is up. The density is shown on east–west and north–south planes through a linear color mapping from a maximum (red) of  $21 \text{ cm}^{-3}$  and a minimum  $0.003 \text{ cm}^{-3}$  (blue).

improvement from using an extended tail in modeling the magnetosphere can be easily seen by comparing the ionospheric patterns with those obtained earlier for northward IMF and average solar wind conditions. With the downstream boundary at  $-100 R_E$  a 2 cell convection pattern in the ionosphere with a cross polar cap potential of about 45 kV was found. Region 1 currents dominated the convection, although weak NBZ currents appear. Conversely, the new code extending to  $-300 R_E$ , shows a 4 cell convection pattern with the NBZ currents dominating, and a cross polar cap potential of roughly 14 kV, consistent with the observations.

Preliminary results from the new code are shown in Figures 2–5. Figure 2 shows the magnetic field structure for northward IMF, which could be considered as the 'ground state' of the magnetosphere. After a few hours of steady northward IMF a

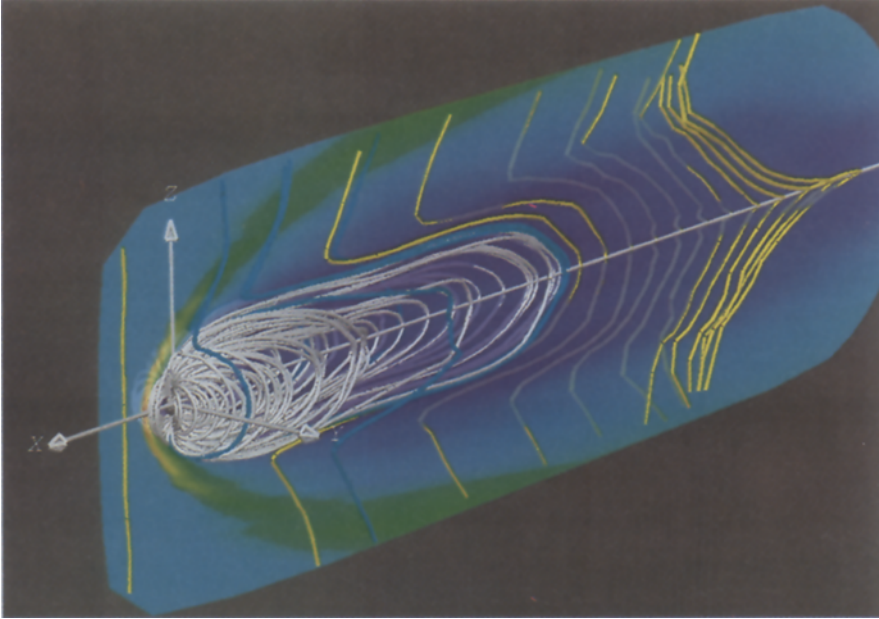


Fig. 2. Magnetic field lines originating from the Earth's dayside hemisphere, and the Sun–Earth axis from an MHD simulation with northward IMF. Closed field lines are shown in white, open (reconnected) field lines in cyan, and solar wind field lines in yellow. The density is shown on a north–south plane through a linear color mapping; the plane is transparent to allow the field structure to be seen.

quasi-static essentially closed, ‘tadpole’ shaped magnetosphere is formed with no Earth connected magnetic flux past  $-155 R_E$ , no open field lines in the lobes, and intermittent reconnection at the cusp regions. In the ionosphere, a 4 cell convection pattern, strong NBZ currents, and a realistically weak cross-polar potential are seen (Fedder and Lyon, 1993). In contrast, for southward IMF strong reconnection on the dayside and in the tail dominate the field structure, limiting the extent of the closed portion of the magnetosphere to  $30\text{--}50 R_E$  (Figure 3). For eastward IMF, an intermediate structure is seen (Figure 4). Reconnection on the dayside shifts at roughly  $45^\circ$  from the elliptic plane and the reconnected field lines are swept tailward and twist around the closed magnetosphere, which extends to perhaps  $100 R_E$ .

In addition the new code has allowed us to realistically study dynamic effects such as the response of the magnetosphere to changes in the solar wind velocity and the windsock effect. In Figure 5, initial results are shown from a simulation in which a radially propagating tangential discontinuity (TD), in which only the transverse plasma velocity is changed, impinges on the magnetosphere (Goodrich and Lyon, 1992). It is seen that the magnetotail does attempt to realign along the new plasma velocity direction, but that the propagation of the response is progressively slower from the flanks to the center of the tail, where it propagates at a speed 20% slower

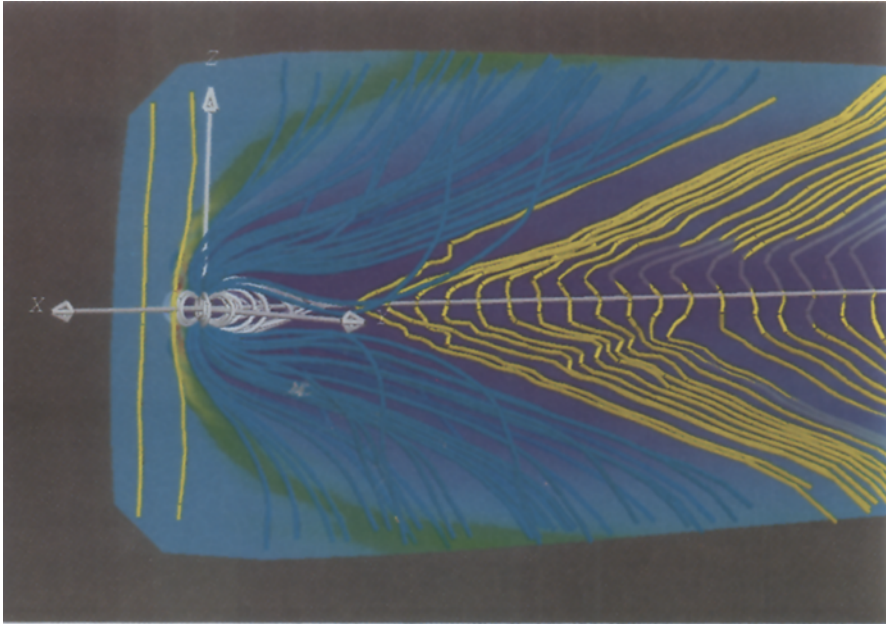


Fig. 3. Magnetic field lines from an MHD simulation with southward IMF. Closed field lines are shown in white, open (reconnected) field lines in cyan, and solar wind field lines in yellow. The plasma density is shown on a north–south plane through a linear color mapping; the plane is transparent to allow the field structure to be seen.

than the TD itself. Since it takes approximately two hours for the response of the center tail to reach  $200 R_E$ , the effects of solar wind variations with time scales 30 min or less could combine nonlinearly in the tail.

### 3. Local Modelling

While global MHD modeling can give a reasonable overall picture of the structure of the solar wind–magnetosphere–ionosphere system, the MHD description breaks down at magnetospheric boundary layers. MHD cannot model scale lengths shorter than a few ion Larmor radii, and cannot describe field aligned or kinetic effects. Such physics is of central importance to the transport of energy through the magnetosphere. The most familiar examples of the inadequacy of the MHD description in the magnetosphere are the bow shock, the magnetopause and the magnetotail. In each case, very short length scales (much less than the resolution of MHD codes) are observed, and collective plasma effects are expected resulting in selective heating and acceleration of different ion species. To model such effects correctly, a full particle treatment is needed for some (or all) of the particle species.

Of course, the ideal solution to this problem is to attempt full particle simulations of the global magnetosphere for the correct parameters. Unfortunately, this is many

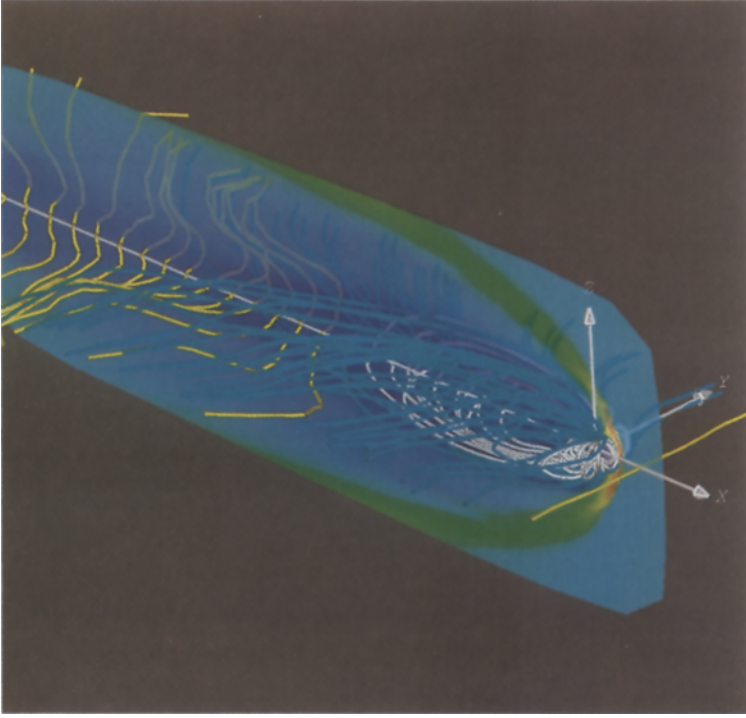


Fig. 4. Magnetic field lines from an MHD simulation with eastward IMF. Closed field lines are shown in white, open (reconnected) field lines in cyan, and solar wind field lines in yellow. The density is shown on a north-south plane through a linear color mapping; the plane is transparent to allow the field structure to be seen.

years (or even decades) in the future. At the present, such particle simulations are restricted to modeling localized regions of the magnetosphere, such as the bow shock, the magnetopause, the magnetotail, the plasma sheet boundary layer, etc. As such, they are performed in isolation from the global magnetosphere. Feedback from, and input to, the magnetospheric system is generally held to a minimum. One of the major goals of our ISTP project is to develop approaches to perform the coupling of the local physical processes to the global models.

Two types of local simulations will be used by the theory groups in the ISTP project. Full particle codes, which treat all species as simulation particles, are discussed by the UCLA group elsewhere in this issue (Ashour-Abdalla *et al.*, 1994). The emphasis of our group is on hybrid codes, which treat the ions as simulation particles and the electrons as a fluid that can have finite inertia if required. While significant physics is lost by using the electron fluid assumption, hybrid codes have the advantage over particle codes that they can model much larger systems without resorting to highly artificial parameters, such as the electron-ion mass ratio, and  $\omega_e/\Omega_e$  (where  $\omega_e(\Omega_e)$  is the electron plasma (gyro) frequency). Both one- and two-dimensional hybrid codes are in use. The 1-D code (e.g., Winske, 1985; Winske and



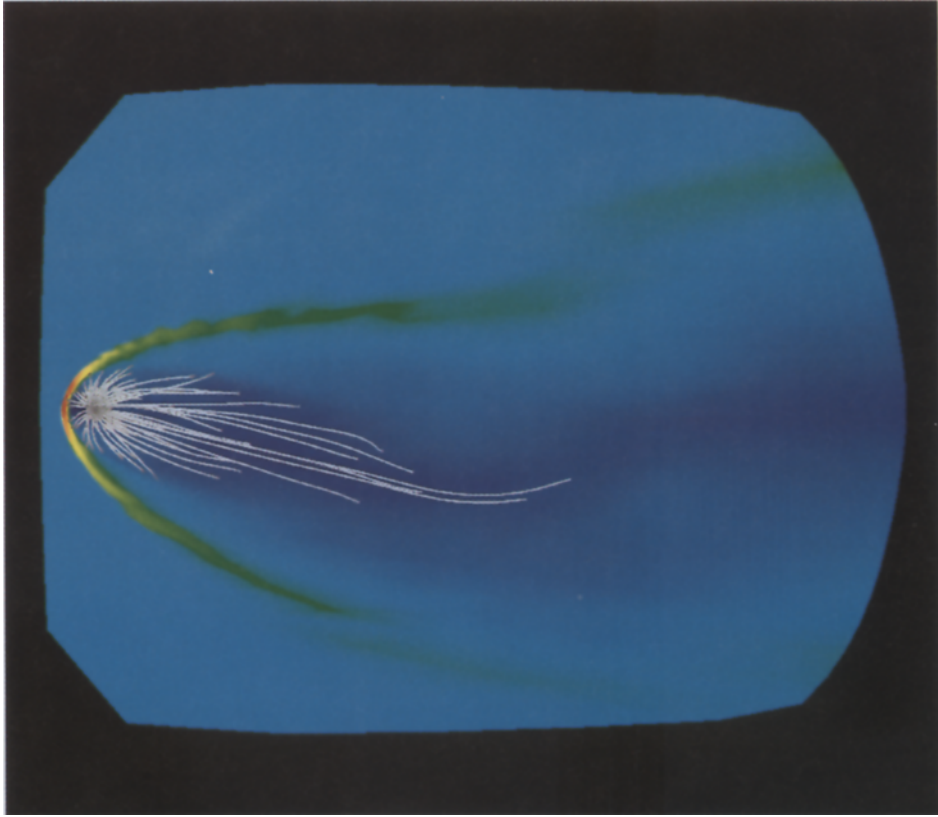


Fig. 5. Density and magnetic field lines originating from the Earth's northern polar region from an MHD simulation with a westward IMF 20 000 s after a tangential discontinuity impinges on the magnetosphere. The density is shown on an east-west plane through a linear color mapping.

Omidi, 1991) treats the electrons as a massless fluid and has been used by our group on problems related to collisionless shocks (Leroy *et al.*, 1982; Papadopoulos, 1985; Cargill and Goodrich, 1987), tangential discontinuities (Cargill, 1990; Cargill and Eastman, 1991) and rotational discontinuities (Goodrich and Cargill, 1991). The 2-D code has been developed in collaboration with Science Applications International Corporation (SAIC). A version of the code, with massless electrons that solves the electromagnetic equations by an explicit scheme (Mankofsky *et al.*, 1987) has been used on beam propagation (Papadopoulos *et al.*, 1988, 1991) and magnetotail problems (Chang *et al.*, 1991). Another version of the code that includes electron inertia and solves the field equations implicitly is currently under development (Mankofsky *et al.*, 1990) and will become operational in the near future. It will enable us to perform simulations over longer time scales (since it is faster than the explicit code) or to examine phenomena such as lower hybrid

waves that require finite electron inertia with appropriate choice of time steps. In the following we discuss some applications of these codes.

### 3.1. MAGNETOPAUSE

The magnetopause is a narrow transition between the shocked solar wind plasma in the magnetosheath and the magnetosphere; its width is estimated to be a few ion Larmor radii. In addition, its structure appears to involve narrow boundary layers of magnetosheath plasma that have penetrated into the magnetosphere. Two simple models of the magnetopause assume that it can be modeled as either a tangential discontinuity (TD) or a rotational discontinuity (RD). The former case corresponds to no flow or field penetrating the magnetopause, so that it can be said to be closed. One-dimensional hybrid simulations of TDs have been performed by Cargill (1990) and Cargill and Eastman (1991). An RD, which propagates relative to the incoming flow at the normal Alfvén speed, could be relevant when reconnection occurs in the vicinity of the subsolar point so that mass and energy can access the magnetosphere directly.

The structure of RDs has been studied with 1-D hybrid simulations (Goodrich and Cargill, 1991). It was found that the net field rotation in the RD is the result of a smooth transition from a right handed rotation to a left handed rotation, in transiting from the upstream state to the downstream state of the discontinuity. This basic structure persists over the wide range of plasma parameters studied, including plasma beta ( $\beta \sim 1$  and  $\beta \ll 1$ ). In the latter case, the wave characteristics underlying the structure are more pronounced due to the formation of prominent upstream and downstream wave trains. Simulations with  $\beta \sim 1$  give very similar results for the RD structure itself, but do not exhibit clear wavetrains. Figure 6 shows time sequences of the  $y$  component ( $B_y$ ) of the magnetic field (lower panel) and of the  $z$  component ( $B_z$ ) (upper panel) directions as a function of the normal coordinate ( $x$ ) for  $\beta \ll 1$ . For this simulation, the angle between the direction of propagation and the upstream magnetic field ( $\theta_{BN}$ ) is  $30^\circ$ , and the initial sense of field rotation is Alfvénic (Goodrich and Cargill, 1991). The total time shown is  $250 \Omega_i^{-1}$ . In Figure 6, time increases in a direction heading into (out of) the page in the upper (lower) panel, so that different features of the RD evolution can be seen. The figure caption gives a full description of the color coding.

The structure of the RD is dominated by the dispersive properties of low-frequency ( $\leq \Omega_i$ ) waves prominent in Figure 6. Fast mode waves have group velocities large enough to travel away from the RD in the upstream direction, forming the upstream wave train, while the slower Alfvén (intermediate) mode waves are convected downstream. The necessity to match two different waves with opposite senses of helicity at the RD gives rise to a very characteristic ‘S’-shaped signature in the magnetic hodograms ( $B_y - B_z$  plots), as shown in Figure 7. While the extended wavetrains do not form for  $\beta \sim 1$ , the same matching of right- and

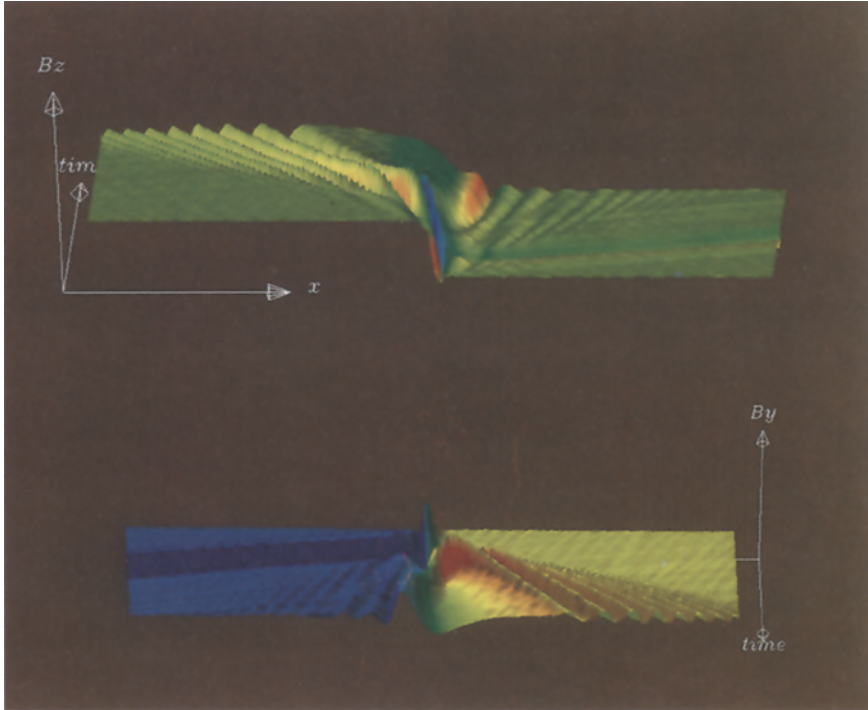


Fig. 6. The temporal evolution of the transverse field components of a rotational discontinuity based on a 1-D hybrid numerical simulation. The simulation extends  $500 c/\omega_i$  in the  $x$  direction and results to  $t = 250 \Omega_i^{-1}$  are shown. In the upper panel  $B_z(x, t)$  is shown as the height of the 3-D surface with value of  $B_y$  linearly scaled to a color map on the surface from  $-5\gamma$  (red) to  $5\gamma$  (blue). A surface, rotated  $180^\circ$ , showing the value of  $B_y$  is shown in the lower panel overlaid with a color map proportional to  $B_z$ . Note that time increases out of the page in the lower panel.

left-handed rotations occurs. Such signatures have been seen in the experimental data in both the solar wind and at the magnetopause.

Future work in this area will be directed toward extending these preliminary calculations to multiple dimensions. Issues of particular interest are whether the wave structures seen in 1-D persist, or whether the introduction of more dimensions makes available other channels that transmit the wave energy. In the more distant future, it is clearly desirable to develop models that take into account the precise conditions on either side of the magnetopause. Existing RD calculations assume that the RD exists in isolation. However, the magnetopause is much more complicated than that, with an array of other discontinuities present on both the magnetosheath and magnetospheric sides of the RD. It is clearly desirable to study the influence of these discontinuities on RDs and *vice-versa*. The development of such a model could then allow realistic comparisons to be made with the CLUSTER mission, which will provide the first ever multi-dimensional picture of the magnetopause.

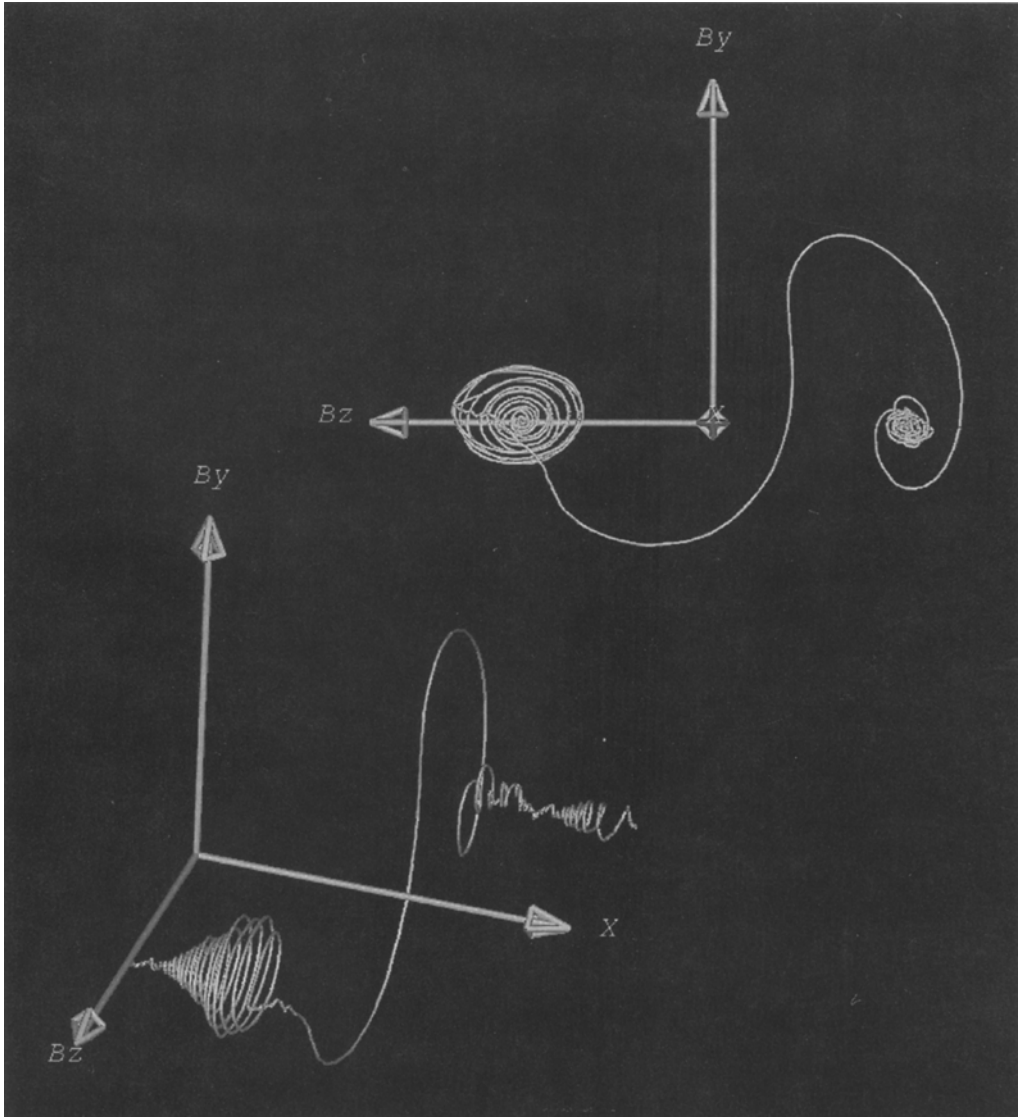


Fig. 7. Two views of the three-dimensional magnetic hodogram ( $B_y$  vs  $B_z$  vs  $x$ ) at  $t = 250 \Omega_i^{-1}$  of the RD simulation shown in Figure 6.  $B_z$  is positive on the upstream side (to the left of Figure 6, upper panel) and negative on the downstream side. Between the upstream and downstream states, the magnetic field traces out a characteristic 'S'-shaped hodogram, which corresponds to a matching of fast and Alfvén waves.

### 3.2. TAIL NEUTRAL SHEET

The structure and stability of the geomagnetic tail is another important problem for which hybrid codes are well suited. Our initial simulations have concentrated on setting up a Harris equilibrium (Chang *et al.*, 1991). Future research will involve studying the evolution of the local tail properties in response to given solar wind conditions, such as the generation of a cross-tail electric field. We are particularly interested in examining whether any reconnection can develop in the simulations (either the ion tearing mode or driven by finite electron inertia effects), since reconnection has long been believed to play a critical role in the initiation of substorms. Data from the ISTP satellites can provide input for such simulations (e.g., at the magnetopause), with the results being compared with the experimental data from both GEOTAIL and CLUSTER.

The nonequilibrium behavior of the magnetotail plasma sheet is central to understanding substorms; the stability of the plasma sheet to a number of different modes has been examined. For example it was shown (Lui *et al.*, 1991) that a kinetic cross-field streaming instability could provide a possible trigger for substorm onset. More recently, the central tail response to compressions induced by the temporal variation of the solar wind flux has been studied. Physically, compression of the plasma sheet results in a mass acceleration toward the neutral line located at the center of the plasma sheet. This acceleration force, denoted by  $g$  for convenience, induces particle drift motion in the direction of  $g \times \mathbf{B}$ , where  $\mathbf{B}$  is the ambient magnetic field in the magnetotail. Such drift motion can cause unstable plasma oscillations that grow exponentially in time and which may lead to plasma turbulence and anomalous resistivity in the plasma sheet (Huba *et al.*, 1990). Another important aspect of the neutral sheet physics currently studied is its response to low frequency perturbations. It was noted (Papadopoulos *et al.*, 1994) that when the neutral sheet thins to a size  $L < c/\omega_i$ , where  $\omega_i$  is the ion plasma frequency the dominant low-frequency response changes from the usual Alfvénic to a helicon (i.e., a whistler with frequency below the ion cyclotron frequency). This can have significant implications since it allows for flux penetration of the order  $V_A(c/\omega_i)L$  where  $V_A$  is the Alfvén speed. A new hybrid model is currently under development to study this effect.

## 4. Nonlinear Dynamical Studies of Magnetospheric Activity

Another part of our project approaches the magnetospheric structure and activity in an unconventional way. It relies on recent developments in the study of far from equilibrium systems, starting with the famous weather model of Lorentz (1963). These developments indicate that even deterministic systems with few degrees of freedom yield complex and irregular dynamics if they are nonlinear and include dissipation. A remarkable property inherent in nonlinear dissipative systems is

that their phase space contracts as they approach the asymptotic state. This state is called an attractor and can, in general, be described by fewer variables than the original system. The magnetosphere is a nonlinear system and exhibits highly irregular behavior as seen in indices measured on the ground, such as the AL, AE, and Dst and in many satellite observations. The presence of strong nonlinearity is suggested by the linear prediction filter analysis of the AL index with respect to the product VBs of the interplanetary magnetic field (Bargatze *et al.*, 1985). Is the magnetosphere a truly random system whose irregular behavior arises from the presence of many degrees of freedom or is it a low dimensional system that, at least in its asymptotic state, can be described by a few nonlinearly coupled differential equations as expected from the presence of an attractor? To decide whether there is a magnetospheric attractor and to determine the number of variables required to describe the magnetosphere we followed the methodology of time series analysis of nonlinear dynamical systems, the relevant aspects of which are described below.

Most observational data are of a few of the many physical variables of the system giving incomplete details of the phase space evolution. However, this difficulty can be overcome if the system variables are sufficiently nonlinearly coupled. In such cases the time delay embedding technique (Grassberger and Procaccia, 1983) is an appropriate method for using time series data to reconstruct the phase space and obtain its characteristic quantities. In this technique we construct a  $m$ -dimensional space, commonly called the embedding space, from the time series data, e.g.,  $x(t)$ . This space can be viewed as representing the actual phase space of the system, *viz.*, the magnetosphere, and a point in it represents the state of the system at a given time. The  $m$ -component state vector  $\mathbf{X}_i$  from a time series  $x(t)$  can be constructed as  $\mathbf{X}_i = \{X_1(t_i), x_2(t_i), \dots, x_m(t_i)\}$ , where  $x_k(t_i) = x(t_i + (k - 1)\tau)$  and  $\tau$  is an appropriate time delay (of the order of characteristic physical time scales). In this reconstructed phase space the distribution of state vectors is directly related to its dimension. The dimension is reflected in the way the points are distributed and can be obtained by examining the scaling of an appropriately defined distribution function with distance. Such a function is the *correlation sum* giving the number of points  $C(r)$  within a specified distance  $r$  of any point. If the number of points is large enough, this distribution will obey a power-law scaling with  $r$  for small  $r$ :  $C(r) \sim r^\nu$ , and the *correlation dimension*  $\nu$  can be defined as  $\nu = \log C(r) / \log r$  in the limit of  $r \rightarrow 0$ . As we increase the dimensionality of the embedding space by increasing the parameter  $m$ , the correlation dimension converges to its true value for an attractor and  $\nu < m$ . However, in the absence of an attractor, the system explores the available state space and  $\nu = m$ , e.g., in the case of random systems. For an attractor, the minimum degrees of freedom is the nearest integer above  $\nu$ .

Recognizing the nonlinear, dissipative and non-equilibrium nature of the global solar wind–magnetospheric system, these techniques were utilized to study the intrinsic properties of the magnetospheric activity, such as seen in substorms. The key feature such a study is the direct use of observational data such as the AE

and AL indices to reconstruct the phase space of magnetospheric activity. To the present time, we have approached this problem in four stages.

In the first stage, the correlation dimension of magnetospheric activity was studied. This gave a fractional dimension of approximately 3.5, showing the low-dimensional behavior and fractal structure of magnetospheric activity (Vassiliadis *et al.*, 1990). In the second stage, the largest positive Lyapunov exponent, which characterizes the divergence of neighboring trajectories leading to chaos, was found to be positive with its inverse of the order 15 min (Vassiliadis *et al.*, 1991). The time scale over which the system becomes chaotic is a few times the characteristic time scale, which agrees well with the results obtained earlier using techniques such as linear prediction filter analysis (Bargatze *et al.*, 1985). In the third stage, a singular system analysis of the AE and AL indices was used to compute the correlation dimension, yielding a value of 2.5. Thus the global magnetospheric dynamics can be described by 3 or 4 variables. This implies that there is a large scale coherence in the global magnetospheric dynamics and the large number of variables are nonlinearly coupled to yield a few effective variables. This result permits us to proceed with the construction of the dynamical equations that describe the low-dimensional magnetospheric activity (Sharma, 1993). This is currently being carried out by considering nonlinear couplings of up to the third order and using the least squares fit to compute the coefficients. In the future the predictability of the equations will be analyzed by comparing the actual data with that generated by the model. In the fourth stage, a prediction algorithm based on the low-dimensional behavior was developed and with 2.5-min averaged AL data it can predict up to 25 steps, corresponding to about 60 min (Vassiliadis *et al.*, 1992). This time scale agrees with the substorm time scale and is also consistent with the predictability expected from the Lyapunov time scale. It implies that the auroral electrojet indices AE and AL, which are good measures of the magnetospheric substorms, cannot be used to predict the dynamical features of substorms beyond 60 min. It should be noted that this limited predictability is a direct result of the chaotic nature of magnetospheric dynamics. (A chaotic deterministic system has the property that its dynamics can be predicted, unlike a random system, but the chaotic nature limits the prediction to a few Lyapunov time scales.) It may, however, be noted that the current techniques of time series analysis yield Lyapunov exponents which may not be as robust as the correlation dimension. It is therefore possible that the magnetospheric dynamics is low-dimensional but not chaotic, in which case the dynamics will be predictable over long time-scales, e.g., many hours. For the chaotic case, predictions on longer time scales are possible using time series data averaged over longer periods, e.g., 1 hour averaged Dst index. However, these longer time-scale predictions will correspond to the dynamics of magnetic storms. Clearly the advent of new sets of data from space and ground ISTP sensors will permit further testing of this approach to the solar wind–magnetospheric coupling.

The importance of the nonlinear dynamical techniques lies in its ability to yield a description of the magnetosphere that embodies the intrinsic characteristics

contained in the observational data, independent of modeling assumptions. The data from the ISTP mission will be used to resolve a number of issues in solar wind–magnetosphere coupling. The solar wind data from SOHO and WIND, and simultaneous data from CLUSTER, will be used to examine the degree to which magnetospheric dynamics is driven. The CLUSTER data are ideally suited to the study of local dynamical behavior and the extent to which different regions are coupled. This will yield the conditions under which a global dynamical description is valid. Similarly the GEOTAIL data along with the simultaneous data from the other spacecraft in the inner magnetosphere will be used to analyze the coupling during geomagnetically active as well as quiet times. The satellite data represent the local behavior of the magnetosphere, while the ground based data such as the AE, AL, and  $D_{st}$  indices represent the global behavior. The dynamical characteristics obtained from the satellite data will be compared with those from the ground-based data to identify the local vs global behavior and the coupling between different regions. These studies complement the MHD simulations by identifying the intrinsic characteristics which may not be evident on the physical variables of the simulation.

## 5. Discussion

The ultimate goal of our project is to synthesize the elements previously described, MHD modeling, local boundary layer studies and analysis via nonlinear dynamical techniques, into quantitative models of geospace. The constant refinement of the computational models and the required analytic input through detailed comparison with the observational data is a crucial part of the project. This synthesis can be best accomplished through a comprehensive simulation that encompasses the entire magnetosphere, while resolving the full microscale physics of the boundary layers; this is not possible now, though it may become so as computers grow in speed and memory size and new computational techniques are developed. A more realistic, but still ambitious method is to incorporate local kinetic codes as dynamic ‘cells’ within the global MHD code to simulate the important regions such as the magnetopause; the kinetic codes communicate through their (time dependent) boundary conditions to the MHD simulations. While we are exploring the feasibility of this approach, it is not ready for productive use at this time.

For the present we follow an interactive multi-level approach. The global MHD code provides the foundation for our quantitative models. We start by performing simulations under a variety of relevant solar wind conditions to benchmark likely cause and effect relationships within the MHD framework. Hybrid kinetic simulations are then performed to understand the local plasma transport and energization processes in key boundary layers such as the magnetopause and the plasma sheet. The parameters of these simulations, including the initial state and boundary conditions, are based on the current MHD results and spacecraft plasma and field



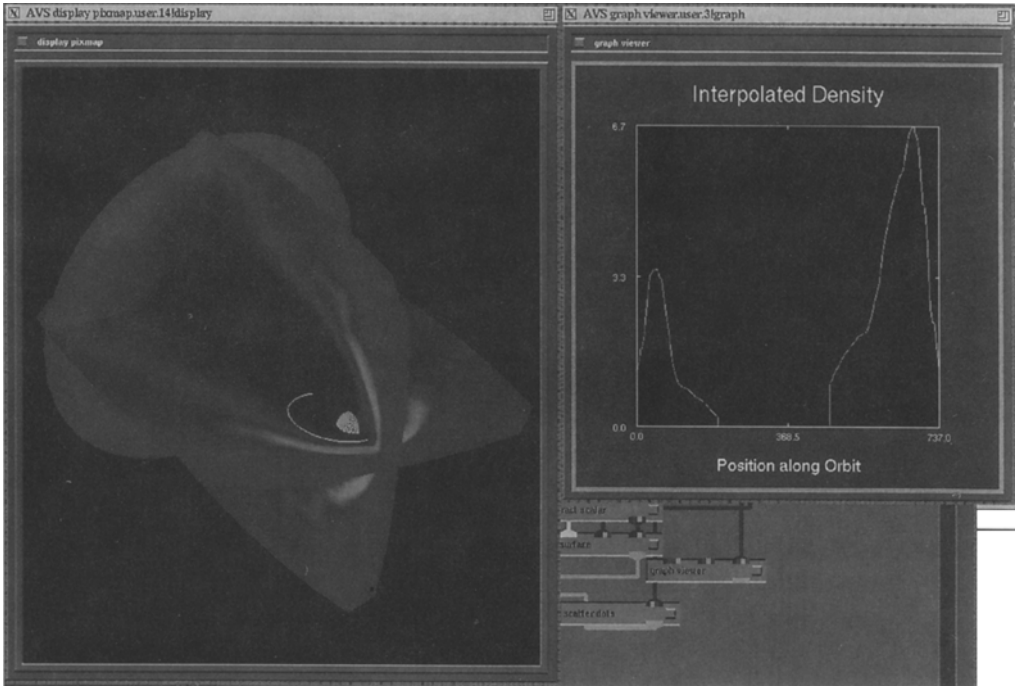


Fig. 8. Example of using AVS to combine MHD simulation results with spacecraft orbits. To the left is a 3-D display of the plasma density from an MHD simulation similar to Figure 1, with a nominal Geotail orbit plotted as a white line. The 1-D plot to the right displays the density interpolated onto this orbit. Different spacecraft and model variables can be chosen interactively and displayed.

data. Analytic theory is also used to plan and analyze the simulation results. Our experience has shown that a strong analytic effort is a prerequisite to the development of reliable computer simulations of complex physical systems. Our results, simulation and analytic, will be tested against the *in situ* data from spacecraft crossing of the boundary layers. These data include ion distribution functions as well as plasma moments and electric and magnetic field data. Local measurements of higher frequency waves (lower hybrid, ion cyclotron, etc.) will also be required to confirm the validity of the derived anomalous transport coefficients. Such spectra are also critical in determining general properties of the turbulent spectra. Another goal of our local modeling is to develop appropriate local transport coefficients, parametrized in terms of the MHD variables, for incorporation in the global simulations. We complete the feedback loop by using these transport coefficients in the MHD simulations to obtain more realistic global results which will presumably provide new aspects for local modelling.

We wish to stress that the interplay of theoretical modeling and observational data is critical to the success of ISTP. The data provide the benchmark needed to validate and refine the models. We plan to use the spacecraft and ground based data available to us through the Central Data Handling Facility (CDHF) of the program to compare with the global and local models in as fine detail as possible.

To achieve this comparison, we are currently building up a data base of global MHD simulations at the CDHF. By varying the solar wind Mach number and plasma beta as well as the angle made by the IMF, we expect to cover a wide range of the data seen by the WIND satellite. To conduct a comparison, an experimentalist need only access the CDHF and give the relevant WIND parameters which will then automatically produce the simulation closest to the WIND input.

We recognize that this detailed comparison is a formidable task involving the coordination of the model results with data sets from numerous experiments on over seven spacecraft positioned through and upstream of the magnetosphere. Furthermore, the direct comparison of the computational predictions with the measured data requires presentation in a common format and appropriate physical units. This is often complicated by the fact that the appropriate model quantities are often implied or derived rather than directly measured quantities. The time honored method of spreading plots of results and data plotted on common scales across a large table is not adequate to handle the complexity of the ISTP program.

We are, thus, developing a method, based on advanced scientific visualization techniques, to analyze the model results and compare them with the data interactively. Fortunately the availability of affordable, powerful scientific workstations combined with the recent advances in interactive data visualization software make this effort practical. We are using a package based on visual programming techniques, the Application Visualization System (AVS) by AVS, Inc., to develop tools to display in three dimension the results of our MHD simulations, show spacecraft orbits within these displays, and to interpolate and plot simulation variables along these orbits together with the appropriate data from the spacecraft. The simulation variables and spacecraft data and orbits are interactively chosen. The modular structure of AVS enable us (and anyone else) to create specialized tools, or modules, that work with the rich set of modules supplied with AVS to build the applications we need. While AVS is a proprietary package, it is available at a moderate cost on most unix workstations, such as will most likely be used widely by ISTP investigators. Figure 8 shows an example of our use of AVS to compare the MHD simulation results with observational data.

### **Acknowledgements**

This work was supported by NASA grant NAG5-1101. Computer resources were provided by San Diego and Pittsburgh supercomputer centers and by the University of Maryland Advanced Visualization Laboratory. Constructive criticism by the reviewers is gratefully acknowledged.

## References

- Ashour-Abdalla, M. *et al.*: 1994, this volume.
- Bargatze, L. F., Baker, D. N., McPerron, R. L., and Hones, E. W.: 1985, 'Magnetospheric Impulse Response for Many Levels', *J. Geophys. Res.* **90**, 6387.
- Cargill, P. J.: 1990, 'Hybrid Simulations of Tangential Discontinuities', *Geophys. Res. Letters* **17**, 1037.
- Cargill, P. J. and Goodrich, C. C.: 1987, 'Shock Wave Interactions in a Collisionless Plasma', *Phys. Fluids* **30**, 2504.
- Cargill, P. J. and Eastman, T. E.: 1991, 'The Structure of Tangential Discontinuities: 1. Results of Hybrid Simulations', *J. Geophys. Res.* **96**, 13763.
- Chang, C.-L., Mankofsky, A., Papadopoulos, K., and Cargill, P. J.: 1991, 'Numerical Simulations of a Dynamically Thinning Magnetotail Plasma Sheet', *EOS* **72**(17), 252.
- Fedder, J. A. and Lyon, J. G.: 1987, 'The Solar Wind-Magnetosphere-Ionosphere Current-Voltage Relationship', *Geophys. Res. Letters* **14** 880.
- Fedder, J. A. and Lyon, J. G.: 1993, 'The Earth's Magnetosphere is 165  $R_E$  Long: or Self-Consistent Currents, Convection, Magnetospheric Structure and Processes for Northward IMF', *J. Geophys. Res.*, submitted.
- Fedder, J. A., Mobarry, C. M., and Lyon, J. G.: 1991, 'Reconnection Voltage as a Function of IMF Clock Angle', *Geophys. Res. Letters* **18**, 1047.
- Fedder, J. A., Lyon, J. G., and Mobarry, C. M.: 1992, 'Currents, Convection, and the Solar Wind-Magnetosphere-Ionosphere Coupling as a Function of IMF Clock Angle', *J. Geophys. Res.*, submitted.
- Goodrich, C. C. and Cargill, P. J.: 1991, 'An Investigation of the Structure of Rotational Discontinuities', *Geophys. Res. Letters* **18**, 65.
- Goodrich, C. C. and Lyon, J.: 1992, 'MHD Simulation of the Windsack Effect', *EOS* **73**, 461.
- Grassberger, P. and Procaccia, I.: 1983, 'Measuring the Strangeness of Strange Attractors', *Physica* **9D**, 189.
- Hain, K. H.: 1987, 'The Partial Donor Method', *J. Comput. Phys.* **73**, 131.
- Huba, J. D., Hassam, A. B., and Winske, D.: 1990, 'Stability of Sub-Alfvénic Plasma Expansions', *Phys. Fluids* **B2**, 1676.
- Leroy, M., Winske, D., Goodrich, C. C., Wu, C. S., and Papadopoulos, K.: 1982, 'The Structure of Perpendicular Bow Shocks', *J. Geophys. Res.* **87**, 5081.
- Lorenz, E. N.: 1963, 'Deterministic Nonperiodic Flow', *J. Atmospheric Sci.* **20**, 130.
- Lui, A. T. Y., Chang, C.-L., Mankofsky, A., Wong, H. K., and Winske, D.: 1991, 'A Cross-Field Current Instability for Substorm Expansion', *J. Geophys. Res.* **96**, 11389.
- Mankofsky, A., Sudan, R. N., and Denavit, J.: 1987, 'Hybrid Simulations of Ion Beams in Background Plasma', *J. Comp Phys.* **70**, 89.
- Mankofsky, A., Antonsen, T. M., and Drobot, A. T.: 1990, *An Implicit Electric Field Algorithm for Quasi-neutral Hybrid Plasma Simulations*, SAIC Technical Report.
- Papadopoulos, K.: 1985, in R. G. Stone and B. T. Tsurutani (eds.), *Mirocinstabilities and Anomalous Transport in Collisionless Shocks*, AGU Geophysical Monograph 34, p. 59.
- Papadopoulos, K., Mankofsky, A., and Drobot, A. T.: 1988, 'Long Range Cross-field Ion Beam Propagation in the Diamagnetic Region', *Phys. Rev. Letters* **61**, 94.
- Papadopoulos, K., Mankofsky, A., Davidson, R. C., and Drobot, A. T.: 1991, 'Ballistic Cross-Field Ion Beam Propagation in a Magnetoplasma', *Phys. Fluids* **B3**, 1075.
- Papadopoulos, K., Zhou, H. B., and Sharma, A. S.: 1994, 'The Role of Helicons in Magnetospheric and Ionospheric Physics', *Comm. Plasma Phys. Cont. Fusion*, in press.
- Sharma, A. S.: 1993, in R. Z. Sagdeev (ed.), *Nonlinear Dynamics of Space Plasma and Modeling in Recent Trends in Nonlinear Space Plasmas*, Am. Inst. Phys., p. 141.
- Sharma, A. S., Vassiliadis, D. V., and Papadopoulos, K.: 1993, 'Low Dimensionality of Magnetospheric Activity from the Singular Spectrum Analysis', *Geophys. Res. Letters* **20**, 335.
- Vassiliadis, D. V., Sharma, A. S., Eastman, T. E., and Papadopoulos, K.: 1990, 'Low Dimensional Chaos in Magnetospheric Activity', *Geophys. Res. Letters* **17**, 1841.

- Vassiliadis, D. V., Sharma, A. S., and Papadopoulos, K.: 1991, 'Lyapunov Exponent of Magnetospheric Activity from AL Time Series', *Geophys. Res. Letters* **18**, 1643.
- Vassiliadis, D., Sharma, A. S., and Papadopoulos, K.: 1992, in T. Bountis (ed.), 'Time-series Analysis of Magnetospheric Activity Using Nonlinear Dynamical Methods', *Chaotic Dynamics: Theory and Practice*, Plenum, New York.
- Vassiliadis, D. V., Sharma, A. S., and Papadopoulos, K.: 1993, 'An Empirical Model Relating the Auroral Geomagnetic Activity to the Interplanetary Magnetic Field', *Geophys. Res. Letters* **20**, 1931.
- Winske, D.: 1985, 'Hybrid Simulation Codes with Applications to Shock and Upstream Waves', *Space Sci. Rev.* **42**, 53.
- Winske, D. and Omid, N.: 1991, in Matsumoto (ed.), 'Hybrid Codes: Methods and Applications', *Lecture Notes for the 4th ISSS*.